Geocarto International

ISSN: 1010-6049 (Print) 1752-0762 (Online) Journal homepage: https://www.tandfonline.com/loi/tgei20

Modelling of land use land cover change using earth observation data-sets of Tons River Basin, Madhya Pradesh, India

Sudhir Kumar Singh, Prosper Basommi Laari, Sk. Mustak, Prashant K. Srivastava & Szilárd Szabó

GEOCARTO INTERNATIONAL
2018, VOL. 33, NO. 11, 1202–1222
https://doi.org/10.1080/10106049.2017.1343390

Modelling of land use land cover change using earth observation data-sets of Tons River Basin, Madhya Pradesh, India

Sudhir Kumar Singh[a], Prosper Basommi Laari[b], Sk. Mustak[c], Prashant K. Srivastava[d] and Szilárd Szabó[e]

[a]K. Banerjee Centre of Atmospheric and Ocean Studies, IIDS, Nehru Science Centre, University of Allahabad, Allahabad, India; [b]Department of Environment and Resource Study, UDS Studies, Tamale, Ghana; [c]School of Studies in Geography, Pt. Ravishankar Shukla University, Raipur, India; [d]Institute of Environment and Sustainable Development, Banaras Hindu University, Varanasi, India; [e]Department of Physical Geography and Geoinformatics, University of Debrecen, Debrecen, Hungary

ABSTRACT
An integrated Markov Chain and Cellular Automata modelling (CA MARKOV), multicriteria evaluation techniques have been applied to produce transition probability. The unsupervised method was employed to classify the satellite images of year 1985, 1995, 2005 and 2015 to meet the magnitude of LULC change. Results showing the spatial pattern of the sub-basin is largely influenced by the biophysical and socio-economic drivers leading to growth of agricultural lands and built-up area in the basin. Simulated plausible future LULC changes for 2025 which is based on a CA MARKOV that integrates Markovian transition probabilities computed from satellite-derived LULC maps and a CA contiguity spatial filter (5 × 5). Further, the fragmentation analysis was performed to check the fragmentation scenario in the year 2025. The result for year 2025 with reasonably good accuracy will be useful to the planners, policy- and decision-makers.

ARTICLE HISTORY
Received 28 February 2016
Accepted 13 June 2017

KEYWORDS
Earth observation; LULC change; cellular automata; Markov chain analysis; India

1. Introduction

Land use/land cover change (LULCC) modelling belongs to a rapidly growing scientific field because LULCC is one of the most important ways that humans influence the environment (Srivastava et al., 2012, 2014). It is also one of the important variables that results in global warming. Sometimes anthropogenic activities lead to the development of unique and diverse habitats. However, when treatments ceases these patches becomes endangered by natural processes. Many LULCC studies on environmental changes using spatial and social approach have been widely investigated. Subsequently, land use activities associated with humans have been recognized as an important driver of environmental change at different spatio-temporal scales (Basommi et al. 2016). Many authors have identified that agricultural, mining and mineral processing activities have extensive effects on the environment and natural resources. These processes involved in removal of vegetation, deforestation and soil displacement have negative impacts on the environment (Singh et al. 2012). Furthermore, few studies suggest that tropical deforestation is associated with population and poverty (Lambin et al. 2001; Geist and Lambin 2002; Carr 2004; Carr et al. 2005; Chomitz et al. 2007). These drivers have high

CONTACT Sudhir Kumar Singh sudhirinau@allduniv.ac.in

rates of deforestation within a country and linked to population growth (Lambin et al. 2001; DeFries et al. 2010). DeFries et al. (2010) found that rural population growth is not associated with forest loss, indicating the importance of urban-based and international demands for agricultural products as drivers of deforestation. Moreover, the tropical deforestation is driven largely by changing economic opportunities linked to social, political and infrastructural changes (Lambin et al. 2001; Jha and Bawa 2006). Intensity of these infrastructure developments presumable will increase in the form of roads, electrification, health services and/or potable water, which attracts land-seeking families, and consolidates occupation. The area witnessed an agricultural intensification (higher levels of fertilizer and pesticide inputs and increased output in quantity or value of cultivated or reared products per unit area and time), due to rapidly developing land scarcity may trigger increase in cropping frequency unmatched by appropriate changes in inputs or management, resulting in a 'stressed' ecosystem with stagnating or declining output. The rate of urbanization is high in the area thus affecting land use changes at other places through the transformation of urban–rural linkages. The large-scale urban agglomerations and extended peri-urban settlements have fragmented the landscapes of such large areas hence many ecosystem processes are threatened (Finenko et al. 2001; Lambin et al. 2001; Bogyó et al. 2015; Deák et al. 2016). Few large industrial and educational cities like Satna and Rewa attract a significant proportion of the rural population by way of permanent and circulatory migration, and the wages earned in the city are often remitted by migrants to rural homelands, in some cases transforming the use of croplands and creating 'remittance landscapes' (Lambin et al. 2001) and for better educational facilities. The other most common reason of land use/land cover change is globalization, it amplifies or attenuates the driving forces of land use change by removing regional barriers and strengthening global at the expense of national connections (Lambin et al. 2001; Meyfroidt et al. 2013). After the globalization era 1990, many parts of India became connected to the world in economical perspective (Srinivasan 2001). The interconnectedness of places and people through, global markets, information, social media and capital flows, and international conventions enhance the land use/land cover change in the region.

A substantial amount of Earth's surface and socio-economic data coupled with the ancillary data is a prerequisite for effective analysis, monitoring and modelling of land cover change. The synoptic data at finer scale are now available using remote sensing (RS) and is widely used by the researchers in the field of LULCC studies (Singh et al. 2010, 2012, 2013, 2015; Srivastava et al. 2013; Szabó et al. 2012) for resource management and planning. RS provides an excellent source of data, from which updated LULC information and changes can be extracted, analyzed and simulated efficiently (Singh et al. 2015). LULC mapping, derived from earth observation data-set, has long been an area of focus for various researchers; recent advances in GIS and RS techniques as well as methods have enabled researchers to model these changes effectively in a short period of time. Cellular Automata–Markov Chain model (CA MARKOV) is a robust approach for spatial and temporal dynamic modelling of LULCC because RS and GIS data can be efficiently incorporated in the process (Kamusoko et al. 2009; Steeb 2011; Singh et al. 2015). Cellular Automata (CA) is a popular technique which works on a logical principle 'what-if scenarios' and uniform grid-based principle. It can be utilized in the management, planning, modelling and simulation of the spatial processes (Wu and Webster 2000; O'Sullivan 2001; Wu 2002; Irwin et al. 2009; Araya and Pedro 2010; Singh et al. 2015). The ability of CA to represent complex systems with spatio-temporal behaviour, drawing from a small set of simple rules and states, makes it suitable for modelling the spatial processes. According to Wang and Zhang (2001), biophysical and socio-economic data can be used to; (1) define initial conditions, (2) to parameterize the CA–Markov model, (3) to calculate transition probabilities and (4) to determine the neighbourhood rules with transition potential maps. In the Markov Chain and Cellular Automata modelling (CA MARKOV), the Markov Chain Model (MCM) component controls temporal dynamics among the LULC classes based on transition probabilities, while the spatial dynamics are controlled by local rules determined either by the CA spatial filter or transition potential maps. The potential application of the CA Markov in land use change modelling has been recognized by many researchers by combining biophysical and socio-economic data for simulation of accurate LULC in plausible future (Wang and Zhang 2001;

Chen 2006; Kamusoko et al. 2009; Guan et al. 2011; Jokar Arsanjani et al. 2011; Memarian et al. 2012; Jokar Arsanjani et al. 2013; Behera et al. 2012; Yang et al. 2014; Singh et al. 2015; Bacani et al. 2016; Yulianto et al. 2016).

The causes of fragmentation and habitat loss can be linked to agriculture and infrastructure development, over-exploitation of natural resources, pollution and invasive species (Semwal 2005). At the landscape level, disturbance is related to patch structure, spatial arrangement, their size and duration (McGarigal and Marks 1995) and can be quantified using the spatial landscape metrics. Landscape metrics are the algorithms designed for quantifying landscape pattern depicting the spatial arrangement of land cover patches over a particular geographic area (McGarigal and Marks 1995; Herold et al. 2003; Singh et al. 2016; Lamine et al. 2017). These landscape and class level metrics can be used to see the impact of anthropogenic activities on natural cover, such as forest (Singh et al. 2014, 2016).

The objectives of the study are (1) to analyze the spatial and temporal changes in 1985–1995–2005–2015, (2) to simulate and predict land use changes for years 2015 and 2025 based on CA MARKOV, (3) to perform fragmentation analysis, so as to enable development practitioners, planners, resource managers and policy-makers effectively manage and tailor intervention for better management to preserve the unique natural characteristics in the study area.

2. Materials and methods

2.1. Study area

Tons river basin has a great significance to states Madhya Pradesh and Uttar Pradesh in India, concerning water resources aspects and the ecological balances (Kumar et al. 2017). The study area Tons River basin (also known as Tamsa River) is a sub-basin of the river Ganga which flows in between the states of Madhya Pradesh (MP) and Uttar Pradesh (UP) in Central India. The Tons river originates from a tank at Tamakund of the Kaimur hills at an elevation of 610 m in Satna district of MP at 23° 57′ and 25° 20′ N latitudes and 80° 20′E to 83° 25′E longitudes (Figure 1) and it joins the river Ganga at Sirsa, about 311 km downstream of the confluence of river Ganga and Yamuna in UP. The total catchment area is 17,617 km^2, out of which 11,974 km^2 lies in MP and the remaining area 5643 km^2 lies in UP.

The study area experiences a subtropical climate where total annual rainfall varies from 930 to 1116 mm/year with mean annual rainfall 1099.2 mm/year and 90% falls during monsoon (June–September) season with maximum numbers of rainy days in the months of July and August. The summer season (May–June) is hot with the daily maximum temperature up to 46 °C while winter season (December–January) is cool with minimum temperatures up to 5 °C and the mean annual temperature is about 25.65 °C. The wind speed in the region varies from 0.43 m/s (November) to 1.29 m/s (June) with predominant wind direction from West to North West. The weather remains dry for all the seasons except monsoon when the humidity is around 80% while mean relative humidity varies from 29 to 80%. The soil type in study area is mainly deep black soil, shallow black soil and the mixed red black soil. The major land use of the area is agricultural land and main crops grown are wheat (major crop), rice, soybean, millets (minor crop) and pluses under popular cropping pattern of wheat–pulses and rice–wheat–pulses. The geology of region shows rocks of Vindhyan system, these are further subdivided into three series namely, the Bhander, the Rewa and the Kaimur (Wadia 1975). The Kaimur series of rocks are composed of the Upper Kaimur sandstone, the Kaimur conglomerate, the Bijaigarh shales, the lower Kaimur sandstone and the suket shales (Yadav et al. 2014).

2.2. Data-sets

Satellite images and socio-economic statistical data were collected as of 1985, 1995, 2005 and 2015. Landsat satellite data-sets of the years 1985, 1995, 2005 and 2015 were employed for land use mapping purposes due to their medium spatial resolution (Table 1). Land cover maps of the years 1985, 1995, 2005 and 2015, were derived from Landsat TM and ETM$^+$ (acquired on 24 August 1985, 1 August 1995, 18 August 2005, and 2015). Furthermore, collateral and ancillary data, such as a digital elevation

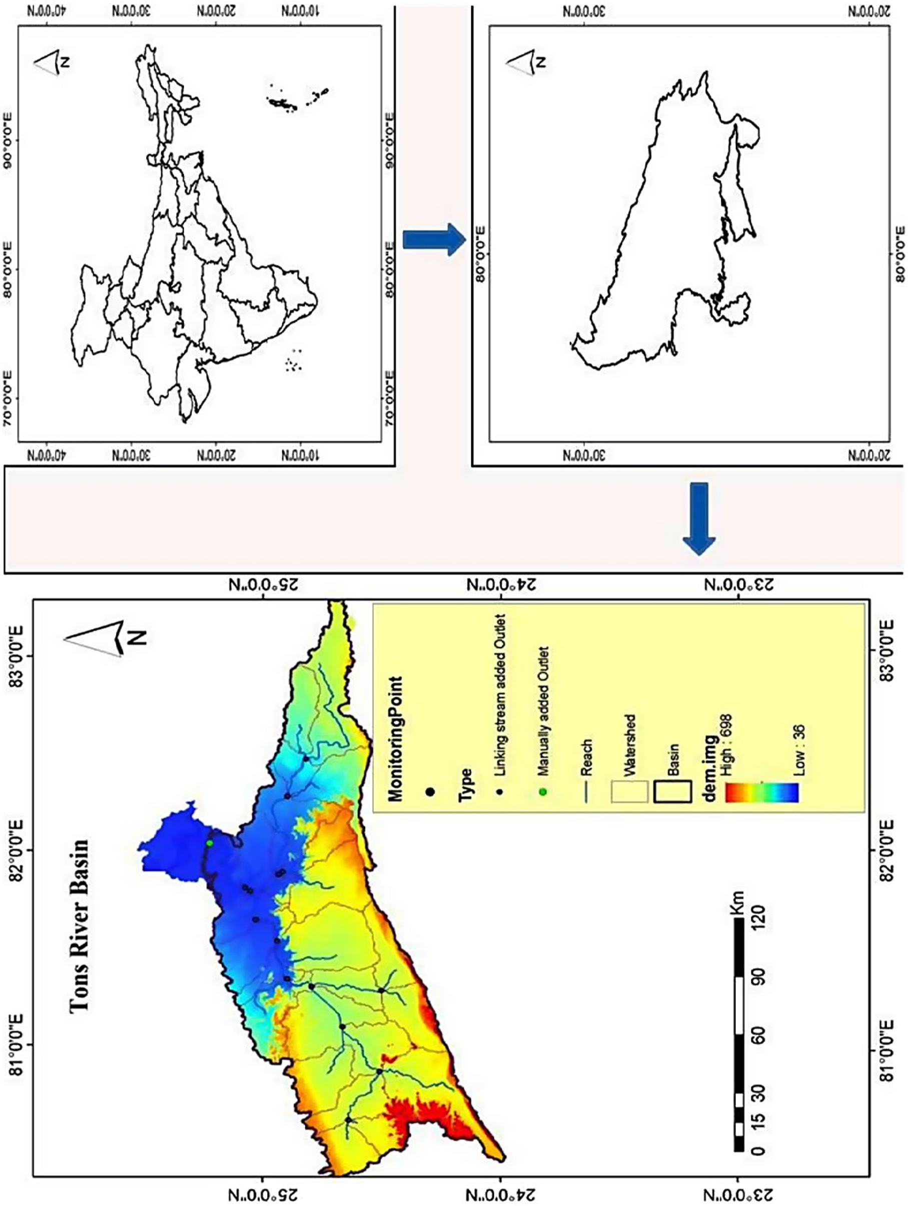

Figure 1. Location map of the study area.

model (DEM) of SRTM, major road networks and images were integrated into the analyses. The adopted methodology of the study is shown by Figure 2.

2.3. LULC map preparation

Classification scheme of Anderson et al. (1976) and National Remote Sensing Centre (2014) was applied to classify the satellite images as deciduous forest, mixed forest, crop land, water bodies, built-up area, fallow and barren land. The LULC classification was performed using unsupervised classification technique because it allows the spectral clustering which gives high degree of objectivity

Table 1. Satellite data specifications.

Year	Satellite/sensor	Spatial resolution (m)	Path/row	Used band combination	Date of data/data access
1985	Landsat, TM	30	142/42, 142/43, 143/42, 143/43, 143/44,144/42,144/43	1, 2, 3, 4, 5, 7	24 August
1995	Landsat, TM	30	142/42, 142/43, 143/42, 143/43, 143/44, 144/42, 144/43	1, 2, 3, 4, 5, 7	1 August
2005	Landsat, ETM$^+$	30	142/42, 142/43, 143/42, 143/43, 143/44, 144/42,144/43	1, 2, 3, 4, 5, 7	18 August
2015	Landsat 8	30	142/42,142/43,143/42,143/43,143/44,144/42,144/43	1, 2, 3, 4, 5, 7	9 June

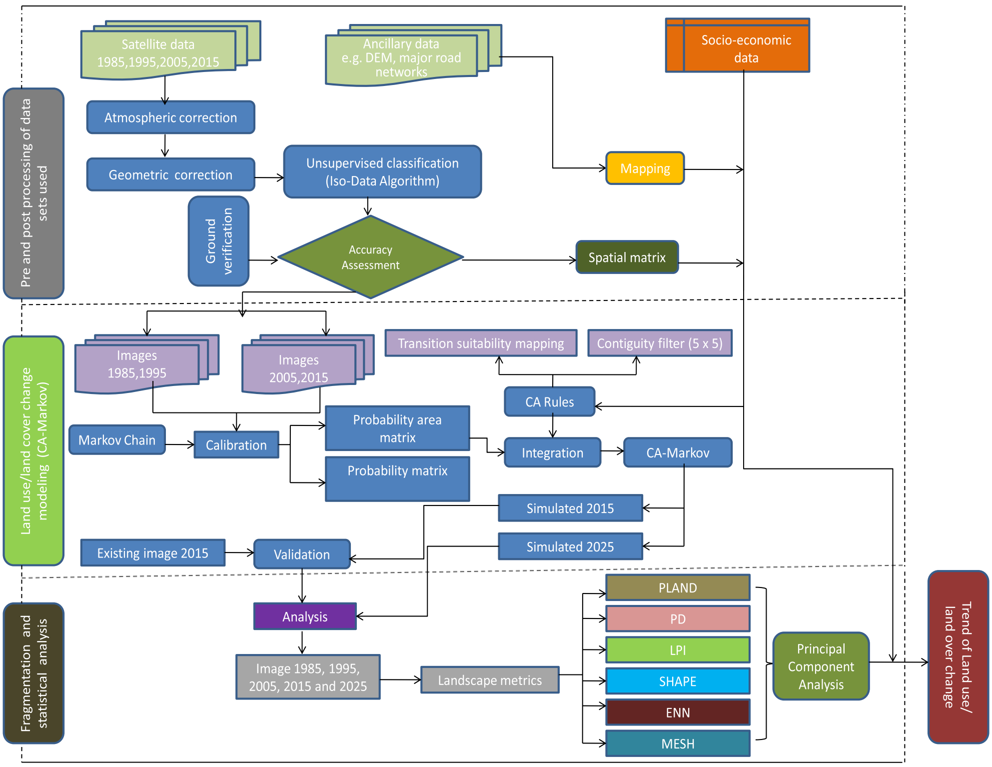

Figure 2. The flow chart is depicting the adopted methodology of the research work.
Notes: The first phase shows the pre- and post-processing of different data-sets used in work, followed by the calibration and validation of CA–Markov model for simulating the plausible future 2025. Subsequently, the fragmentation was studied for 1985, 1995, 2005, 2015 and 2025 to know the trend of land use land cover after calculating the landscape metrics.

without prior knowledge or training site data-sets of the study area. The classified maps for practical purpose need the accuracy assessment and therefore classification accuracy assessment was performed for each LULC maps based on the collected ground control points using Garmin eTrex@ 10 Global Positioning System (GPS) with ±15 m positional accuracy and addition information from public domain software i.e. Google Earth. The regular field visits and surveys were made for the collection of ancillary, collateral data. The spatial layers of ancillary database including different socio-economic and biophysical drivers of LULC change were prepared using data from Indian Census, statistical

Table 2. Socio-economic and physiognomic data used in the study.

Sl. No.	Data type	Year of data	Data source
Socio-economic data			
1	Population	1981,1991, 2001, 2011	Census of India (http://censusindia.gov.in/)
2	Residential and industrial development	1981,1991, 2001, 2011	Statistical handbook
3	Topographic sheets	Topo map and reference map, Survey of India (SOI), India (www.surveyofindia.gov.in)	
4	Total area under summer and winter crops	1981,1991, 2001, 2011	Statistical handbook
Physiognomic data			
1	Drainage network	SRTM DEM (http://www.cgiar-csi.org/)	
2	Slope	SRTM DEM (http://www.cgiar-csi.org/)	
3	Soil map	Food and Agriculture Organisation (FAO) Rome, Italy, National Bureau of Soil Survey and Land Use Planning (NBSS &LUP), Nagpur, Maharashtra, India (https://www.nbsslup.in/)	
4	Geological maps	Geological Survey of India, India (http://www.portal.gsi.gov.in)	

handbook and various other government agencies (Table 2). The CA MARKOV with MCE approach was employed for the prediction of the future LULC dynamics in the sub-basin.

2.4. Accuracy assessment

The accuracy assessment of the different thematic maps produced was checked from the classifiers. It was performed based on the computation of the error matrix statistics (Congalton and Green 1999). As a result, the overall accuracy (OA), user's accuracy (UA), producer's accuracy (PA) and the kappa coefficient (Kc) were computed, using (Congalton and Green 1999) following expressions (1–4):

$$\mathrm{OA} = \frac{1}{N}\sum_{\imath=1}^{r} n_{ii}, \tag{1}$$

$$\mathrm{PA} = \frac{n_{ii}}{n_{i\mathrm{col}}}, \tag{2}$$

$$\mathrm{UA} = \frac{n_{ii}}{n_{i\mathrm{row}}}, \tag{3}$$

$$K_c = N\sum_{\imath=1}^{r} n_{ii} - \sum_{\imath=1}^{r} \frac{n_{i\mathrm{col}}n_{i\mathrm{row}}}{N^2} - \sum_{\imath=1}^{r} n_{i\mathrm{col}}n_{i\mathrm{row}}, \tag{4}$$

where n_{ii} is the number of pixels correctly classified in a category; N is the total number of pixels in the confusion matrix; r is the number of rows; and $n_{i\mathrm{col}}$ and $n_{i\mathrm{row}}$ are the column (reference data) and row (predicted classes) total, respectively.

3. Land use/land cover change modelling

3.1. CA–Markov chain model description

The CA MARKOV describes the probability of land cover change between previous (t1) and later time (t2) periods by developing a transition probability matrix between them (Jokar Arsanjani et al.

2011, 2013; Singh et al. 2015). The probabilities may be accurate on a per category basis, but there is no knowledge of the spatial distribution of occurrences within each land cover class, therefore to incorporate the spatial character to the model, CA is integrated into the Markovian approach. The CA allows the transition probabilities of one pixel to be a function of the adjacent pixel. Developing a transition probability matrix for each of the land cover classes between the years 2005 and 2015 was the first step, and this in turn was used as an input for modelling land cover change. In addition, two types of criteria (constraints and factors) were developed for the determination of suitable lands to be considered for further development (Jokar Arsanjani et al. 2011, 2013). The Boolean character such as 0 and 1 were used for the standardization of the constraints and the factors were standardized to a continuous scale of suitability from 0 (least suitable) to 255 (most suitable). Existing built-up areas and water bodies are the two constraints for the standardization. These constraints were standardized into continuous variables by applying Sigmoidal, J-shaped and linear functions. A transition suitability image collection was developed using the suitability maps derived from the two criteria using the scaling approaches.

3.2. Suitability analysis

Suitability means quality of having the properties that are appropriate for the specific purposes and suitability analysis is a process which identifies the most appropriate spatial pattern of future LULC according to purpose. The criteria for different LULC categories would have different suitability like the criteria for urban suitability would be different than agricultural suitability due to which in each case the suitable places have different features (Malczewski 2004). In the present study, the suitability of urban expansion and its impacts on other land use categories have been assessed.

3.2.1. Multicriteria evaluation

According to Pontius and Schneider (2001), the multicriteria evaluation (MCE) approach is a decision support tool used in GIS to combine the variables with different methodologies which intern transformed into suitability map output. Practically, it is impossible to find a single solution for multiple objective problems of any area that can fulfil all of the objectives simultaneously. In case of any alteration induced due to increase in population or development, we need to take decisions which may include site selection or land allocation decisions that can satisfy multiple objectives, each relating to its own suitability level of land conversion (Soe and Le 2006; Behera et al. 2012). In order to achieve the objectives used MCE approach that deals with the situation in which a single decision-maker is faced with a multiplicity of usually incompatible criteria or in which a number of decision-makers must consider criteria, each of which depends on the decision of the decision-makers (Ademiluyi and Otun 2009). The criteria weight for each land use category was obtained from pairwise comparison matrix of Saaty (1980) using geometric mean method whose sum is equal to 4. Finally, suitable maps of each LULC categories were prepared in MCE module using Weight Linear Combination (WLC) algorithm incorporated with criteria classes, criteria weight and constraints (Figure 3a). WLC method is simply a weighted overlay operation of the different criterion. The main part of the process is the weight allocation to the factors and application of these factors and constraints during the overlay analysis.

The fuzzy set membership approach was used for the standardization of the factors. In suitability analysis, the fuzzy logic helps us to standardize the variables, especially when we deal with the proximity issue (Jiang and Eastman 2000). The fuzzy set functions may be Sigmoidal, J-shaped and Linear, and for this study monotonically increasing linear membership function was applied (Eastman 2009). The weight decision was applied according to the probability of transition of land. The application of MCE technique requires criteria development for decision-making about various land uses. In this study, we integrated different types of data viz. socio-economic data with biophysical data of sub-basin through MCE technique using main criterions Factors and Constrains.

This work utilized two constraints mainly existing settlement and water bodies, because generally new developmental activities cannot thrive on the water bodies and existing settlement areas. The

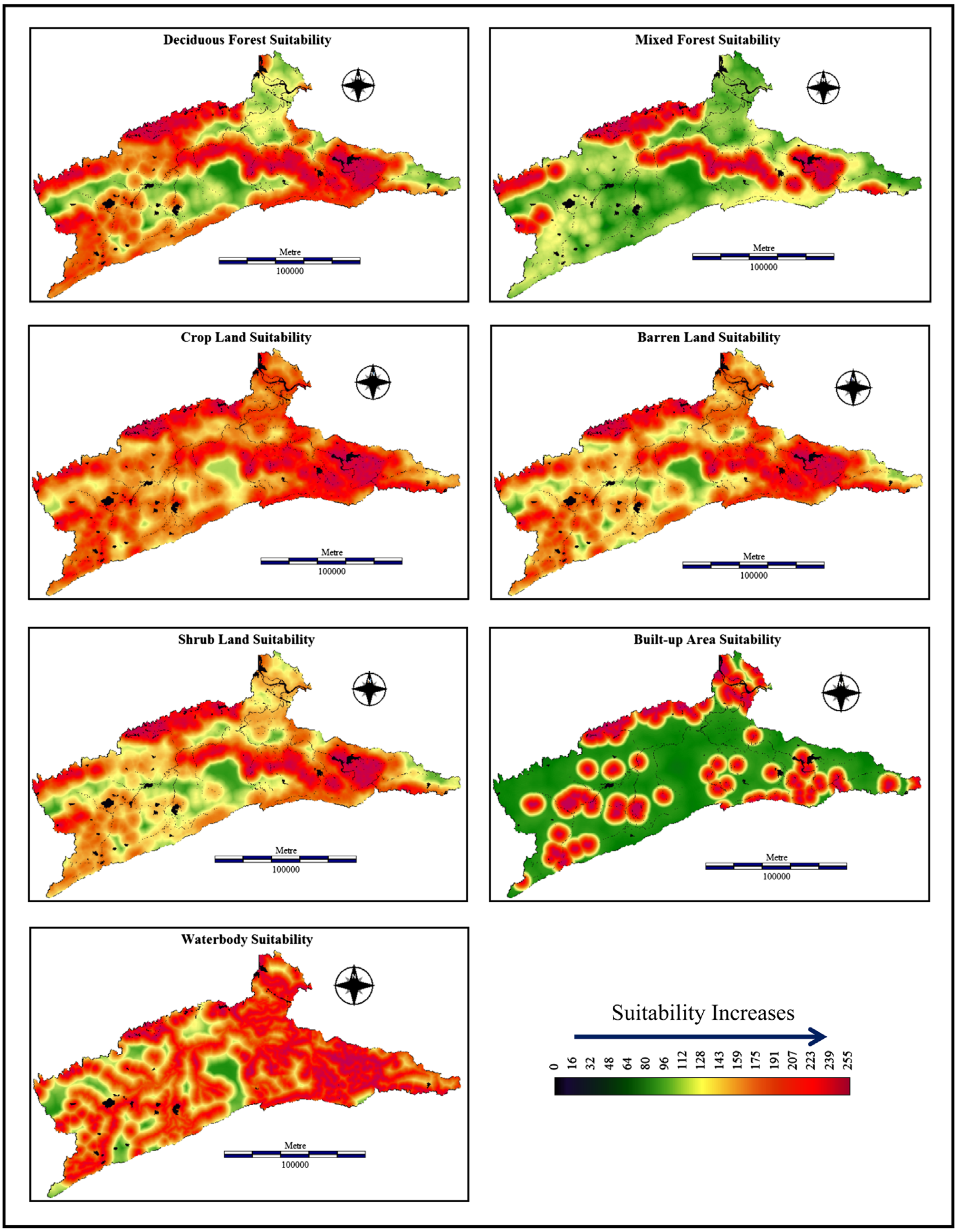

Figure 3a. Transitional Suitability maps for different LULC classes using MCE module (Weight Linear Combination Method, WLC).

water bodies are considered as a constraint for all the LULC classes of the study area except water body. These constraints were expressed in the form of a Boolean map in which areas excluded from consideration were coded with zero and those included for consideration were coded with one as shown in the Figure 3b. Further these images were added up to produce a single suitability image for each land class. Here total five different factors were considered as driving forces or decision variables

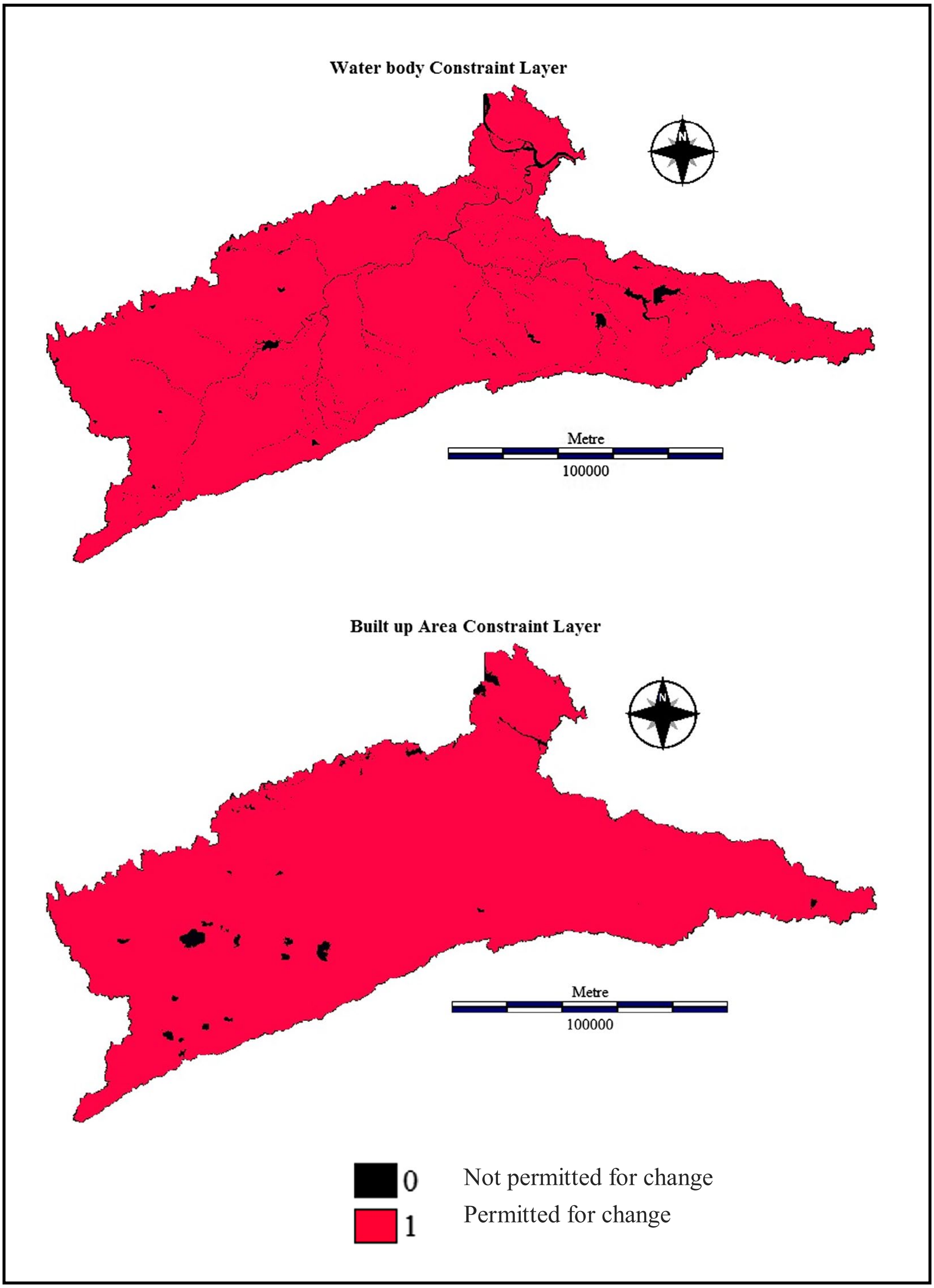

Figure 3b. Constraints of built-up & water bodies using MCE module (Boolean intersection method, BIM).

for LULCC, viz. population, settlement, residential development, industrial development, agricultural expansion, slope, drainage network and different associated LULC classes and the WLC technique in MCE was used.

4. Implementation and validation of the model

Model calibration and validation is an important step (Singh et al. 2015) in any modelling process although there is no consensus on the criteria to assess the performance of land use change models. One way to quantify the predictive power of the model is to compare the result of the simulation (2015) to a reference or real map (2015) using Kappa variations (Singh et al. 2015): Kappa for no information (Kno), Kappa for location (Klocation) and Kappa for quantity (Kquantity). Kno, which is variation of the standard Kappa index of agreement, provides the overall accuracy of a simulation run. The other two indices Klocation and Kquantity, validate the simulations ability to predict location and quantity, respectively (Pontius and Schneider 2001). The simulation's success rate is perfect when Kno, Klocation and Kquantity are equal to 1 and if these indices values are equal to 0 it means the simulation's success rate is imperfect or unsatisfactory (Pontius 2000). Kno indicates the proportion classified correctly relative to the expected proportion classified correctly by a simulation with no ability to accurately specify the quantity or location. Klocation represents the success due to a simulation's ability to specify location divided by the maximum possible success due to a simulation's ability to specify location perfectly. Kquantity is defined as a measure of validation of the simulations to predict quantity perfectly. The predictive power of a model is considered strong when its efficiency is greater than or equal to 80% and then it is useful to make future projections (2025) assuming that the transition mechanism verified between 2005 and 2015 is going to be repeated.

5. Landscape fragmentation analysis

We revealed the trend of changes of LULC types with standardized Principal Component Analysis (PCA) (where calculation was conducted with the correlation matrix of the variables). Percentage of Landscape (PLAND), Patch Density (PD), Largest Patch Index (LPI), Shape Index (SHAPE), Euclidean Nearest Neighbour Distance (ENN) and Effective Mesh Size (MESH) were involved in the analysis as the indices of area, shape, and distance and fragmentation metrics were computed with the help of FRAGSTAT3.3 (McGarigal et al. 2002). PCA reduced the number of variables (i.e. landscape metrics) and Varimax rotation was used to obtain uncorrelated principal components (PC). Numbers of PCs were determined by the Kaiser's rule retaining those ones which eigenvalue was 1< (Jolliffe 2002). These metrics values were used to delineate the component scores and distinguished both the dates and the land cover types. The SPSS 22 used for the statistical calculations.

6. Result and discussion

6.1. Existing land use/cover change

LULC change dynamics of Tons river basin was studied for during the period of 1985–1985–2005–2015. The study area has witnessed increased urbanization and change in different LULC. The results of the accuracy assessment of the classified imageries of the year's 1985, 1995, 2005 and 2015 indicates that the land use changes have been accurately identified and extracted during the classification, which is also confirmed by the overall accuracies and Kappa indices (Table 3). The overall results of LULC distribution for years 1985, 1995, 2005 and 2015 shows that the crop land (CL) is the primary dominant land cover category (Table 4) followed by the deciduous forest (DF) which is the secondary dominant land cover category in the study area. The deciduous forest shows an overall decreasing trend, while mixed forest (MF) shows the increasing trend over the study period. There has been a significant increasing trend observed in the built-up land (BU). More precisely (Table 4), the built-up

Table 3. Accuracy assessments of classified LULC maps for the years 1985, 1995, 2005 and 2015.

	1985		1995		2005		2015	
LULC classes	Producer's accuracy (%)	User's accuracy (%)	Producer's accuracy (%)	User's accuracy (%)	Producer's accuracy (%)	User's accuracy (%)	Producer's accuracy (%)	User's accuracy (%)
Deciduous forest	84.62	91.67	91.67	93.33	85.71	85.71	93.33	87.50
Mixed forest	100.00	80.00	66.67	76.92	71.43	83.33	72.73	94.12
Crop land	94.12	87.67	93.06	89.33	87.06	93.67	96.67	95.08
Barren land	66.67	100.00	66.67	66.67	96.67	70.73	90.91	83.33
Shrub land	35.71	100.00	46.67	70.00	50.00	80.00	62.50	27.78
Built-up	96.88	73.81	83.33	80.00	100.00	100.00	100.00	88.89
Water body	70.03	93.33	100.00	80.00	90.91	100.00	100.00	100.00
Overall accuracy	85.09		83.95		86.88		83.85	
Kappa accuracy	0.7964		0.7809		0.8051		0.7993	

area increased from 52.46 km^2 in 1985 to 74.13 km^2 in 1995, 99.85 km^2 in 2005 to 454 km^2 in 2015. This increase probably took place due to increase in population, widening of highways, set up of new small and large-scale industries in the region and also mining activities for cement material. The deciduous forest area decreased from 2842.50 km^2 in 1985 to 2825.22 km^2 in 1995, 2784.30 km^2 in 2005 and continued to decrease 2524 km^2 in 2015. This decrease in areal extent of deciduous forest is mainly due to its partial conversion into crop land to improve the sustainability of local people of the region and also the conversion into mixed forest. The mixed forest area is 110.07 km^2 in 1985, 185.82 km^2 in 1995, 191.37 km^2 in 2005 and 1732 km^2 in 2015. The increase in mixed forest area is due to conversion of deciduous forest into mixed forest and also due to afforestation in the barren land. The crop land showed the continuous decrease 13,271.71 km^2 in 1985, 13,248.04 km^2 in 1995, 13,252.49 km^2 in 2005 and 11,309 km^2 in 2015, this is due to conversion of crop land into other classes. This may be due to classification error. The area of barren land has decreased from 459.58 km^2 in 1985 to 450.65 km^2 in 1995, 481.10 km^2 in 2005 and further decreased up to 343 km^2 in 2015, which can be attributed to conversion into crop land, urbanization, some reforestation and industrial activities. The shrub land has area of 1239.47 km^2 in 1985, 1165.91 km^2 in 1995, 1178.52 km^2 in 2005 and 1453.94 km^2 in 2015. The shrub land showed slight increase in total area mainly due to conversion of other land use land cover classes into shrub land. Some change in water body class was also seen, which increased from 285.12 km^2 in 1985 to 311.15 km^2 in 1995 and again it showed decreased in area 273.29 km^2 in 2005 and again increased to 445 km^2 in 2015. This increase in water body is due to more number of water tanks and ponds in the region. Overall deciduous forest continues to decrease 2322.75 km^2 in 2025, mixed forest areas increase 252.91 km^2 in 2025, crop land projected to decrease 11,531.4 km^2 in 2025 is due to expansion of national highways, road and cities. The shrub land area will increase to 1459.47 km^2 in 2025. The model has estimated the increase in water bodies total area 1196.41 km^2 in 2025; this probably may be due to creation of new dam, check dam and emergence of other water storage structure in the region. The built-up area will increase to 852.16 km^2 in 2025, due to widening of road, more horizontal expansion of cities and set up of industries. Studies by Temesgen et al. (2017) in Geleda catchment and Solomon et al. (2014) in Koga watershed also reported the growth of cultivated lands at the reduction of forest cover in the respective study periods.

6.2. Land cover modelling and validation

Analysis of the modelling results (Figure 4(a)–(f)) showed that the simulated map for the year 2015 is reasonably similar to the satellite derived map of 2015. A more detailed analysis was accomplished using the Kappa variations. The closer the values of these indices are to 100%, the stronger the agreement is between two maps. The Kno, which also gives the overall accuracy of simulation,

Table 4. Temporal distribution of LULC of years 1985, 1995, 2005, 2015 (real), 2015 (simulated) and 2025 (projected).

Sr. no	LULC classes	1985 (area in Km^2)	1985 (%)	1995 (area in Km^2)	1995 (%)	2005 (area in Km^2)	2005 (%)	2015 (Real) (area in Km^2)	2015 (%)	2015 (Simulated) (area in Km^2)	2015 (Simulated) (%)	2025 (area in Km^2)	2025 (%)
1	Deciduous forest	2842.50	15.56	2825.22	15.47	2784.30	15.24	2524	13.82	2410.99	13.20	2322.75	12.71
2	Mixed forest	110.07	0.60	185.82	1.01	191.37	1.04	1732	9.49	330.60	1.81	252.91	1.38
3	Crop land	13271.71	72.67	13248.04	72.54	13252.49	72.57	11,309	61.93	11733.17	64.25	11531.4	63.14
4	Barren land	459.58	2.51	450.65	2.46	481.10	2.63	343	1.88	397.71	2.17	645.82	3.53
5	Shrub land	1239.47	6.78	1165.91	6.38	1178.52	6.45	1453.94	7.96	1895.83	10.38	1459.47	7.99
6	Built-up land	52.46	0.28	74.13	0.40	99.85	0.54	454	2.48	568.32	3.11	852.16	4.66
7	Water body	285.12	1.56	311.15	1.70	273.29	1.49	445	2.44	924.30	5.06	1196.41	6.55
Total		18260.94	100	18260.94	100	18260.94	100	18260.94	100	18260.94	100	18260.94	100

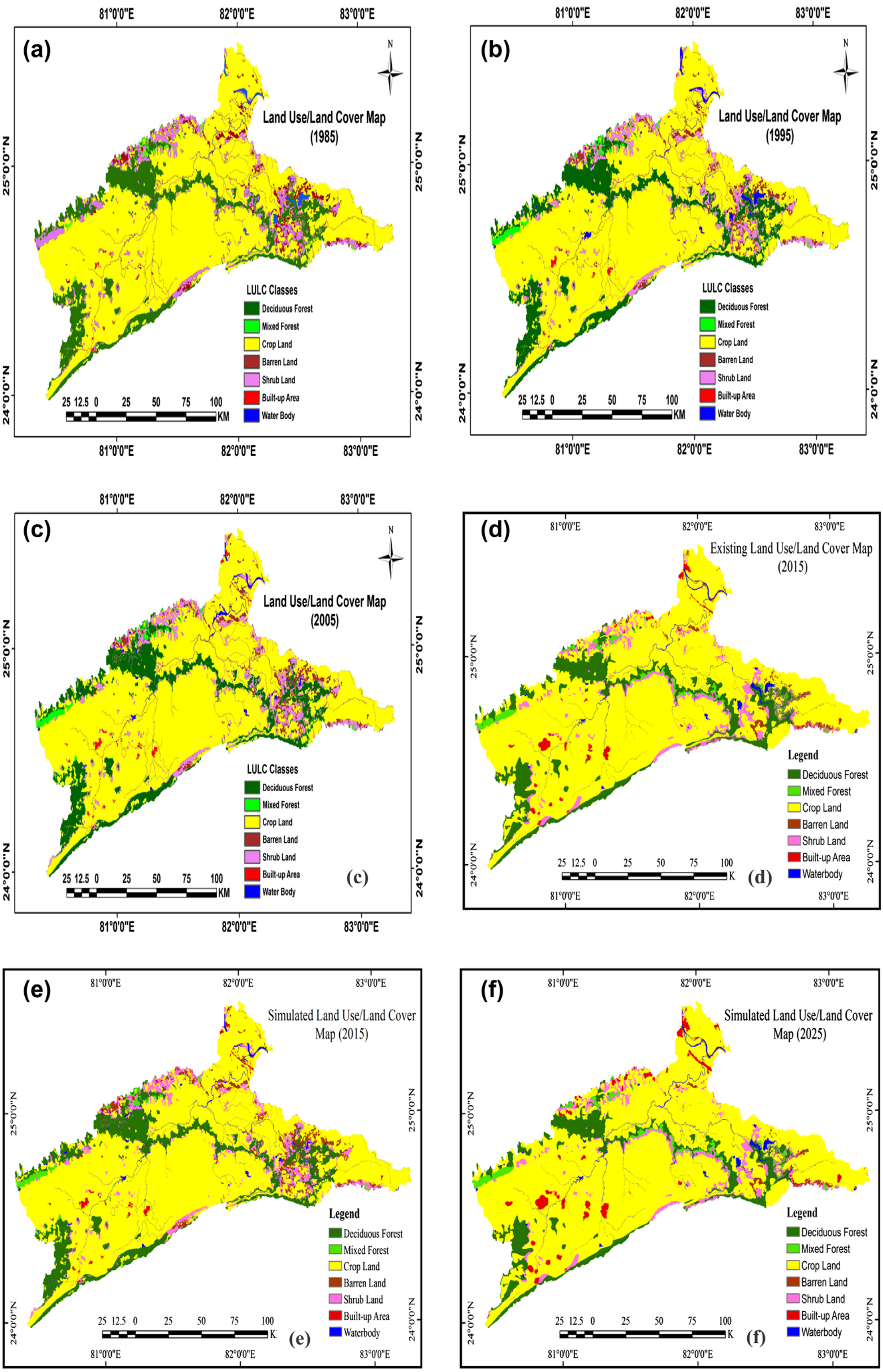

Figure 4. (a–e) Land use land cover map of year of 1985, 1995, 2005, 2015 (real), 2015 (predicted) and 2025 (predicted), the dominant class is crop land.

is calculated to be 79.67%. The model performed very well in the ability to specify location correctly (KlocationStrata = 65.87%), and Kstandard 58.85% and also in the ability to specify quantity (Kquantity = 87.95%). It is important to note that some discrepancies are evident between the real and simulated land cover maps of 2015. This could be due inadequate suitability maps for modelling the phenomenon, generalizations applied for image classification results and the shape of the contiguity filter used. The suitability maps have been used as rules during the modelling process and have had a great influence on the result. Results are also sensitive to the constraints and factors employed to define the rules. After defining the parameters used for the calibration and modelling and assessing the validity, it was interesting to examine the pattern and tendency of change in a long-term simulation. Therefore, land cover projection for 2025 was performed in the same way. A cross-tabulation that describes the changes in land cover classes (Table 5). CA–Markov model has the ability to simulate transition among any number of classes and the nature of the simulation is bidirectional. Two classes (BL and WB) are not included in the matrix because the model did not predict any changes for 2025. The diagonal of the matrix indicates the number of pixels that have persisted during the simulation, while the off-diagonal shows the number pixels that changed for each class.

6.3. Simulated land use land cover change

6.3.1. LULC transition probabilities and transition matrix of year 2015 (simulated)

A transition area matrix records the number of cells or pixels that are expected to change from each LC class to the other over the next period of time. The transition probability presented in Table 6 shows that the deciduous forest has 98.44% probability of remaining as deciduous forest and very low probability to change into other classes. The mixed forest shows 99.96% probability to remain as mixed forest it suggests that this class is very much stable due to application of conservation measure and proper management of forest. The probability for crop land to remain as crop land is 99.54% while its probability to change in shrub land, built-up and water bodies are having very low probability to change, respectively. The probability of change of barren land into 99.64% shows that is stable class. The shrub land has 97.09% probability to remain as shrubland. The built-up shows 100% probability to remain as built-up. The water bodies have 73.65% probability to remain as water bodies. The water body class has high chance to change into other classes. Table 7 explains the expected transition in 2015 in number of pixels of each class to other classes.

Table 5. Classification agreement/disagreement according to ability to specify accurately quantity and location.

	Information of quantity		
Information of location	No [n] None	Medium [m]	Perfect [p]
Perfect[P(x)]	P(n) = 0.3814	P(m) = 0.9549	P(p) = 1.0000
PerfectStratum[K(x)]	K(n) = 0.3814	K(m) = 0.9549	K(p) = 0.9772
MediumGrid[M(x)]	M(n) = 0.3222	M(m) = 0.8258	M(p) = 0.8158
MediumStratum[H(x)]	H(n) = 0.1429	H(m) = 0.5765	H(p) = 0.6005
No[N(x)]	N(n) = 0.1429	N(m) = 0.5765	N(p) = 0.6005

Table 6. Probability of LULC changes in 2015 in percentage.

2005/2015	DF	MF	CL	BL	SL	Built-up	W
DF	0.9844	0.0007	0.0062	0.0004	0.0037	0.0006	0.0041
MF	0.0001	0.9996	0.0000	0.0000	0.0000	0.0000	0.0003
CL	0.0000	0.0001	0.9954	0.0002	0.0005	0.0015	0.0022
BL	0.0000	0.0000	0.0000	0.9964	0.0035	0.0001	0.0000
SL	0.0027	0.0020	0.0131	0.0061	0.9709	0.0025	0.0027
Built-up	0.0000	0.0000	0.0000	0.0000	0.0000	1.0000	0.0000
W	0.0000	0.0001	0.1028	0.0676	0.0902	0.0028	0.7365

Table 7. Expected to transition in 2015 in number of pixels.

2005/2015	DF	MF	CL	BL	SL	Built-up	W
DF	3,045,383	2035	19,300	1172	11,316	1728	12,742
MF	13	212,559	2	0	0	0	66
CL	6	1595	14,657,790	3138	7279	22,634	32,544
BL	0	0	1	532,626	1861	68	0
SL	3548	2597	17,165	8035	1,271,370	3210	3544
Built-up	0	0	0	0	0	110,947	0
W	12	21	31,220	20,517	27,405	840	223,646

6.3.2. LULC transition probabilities and transition matrix of year 2025 (Future LULC)

Tables 8a, 8b shown below demonstrates the number of pixels that are expected to change from 2005 to 2025. Two classes (barren land and water body) are not included in the matrix because the model did not predict any changes for 2025. The diagonal of the matrix indicates the number of pixels that have persisted during the simulation, while the off-diagonal shows the number pixels that changed for each class.

From Table 8a, 64.31% of the dense forest probability will remain as dense forest which signifies its stability though it has 22.80% probability to change into the crop land and 7.97% probability to change into shrub land which would be a result of the increasing demand of food, fodder and fuel by the growing population of the region. The probability of mixed forest to remain as mixed forest is 42.53% though it shows a 23.30% probability of change into crop land and 14.92% to become deciduous forest. Crop land has as high as 92.33% probability to remain as crop land however it has 1.17% probability to change to built-up, 3.17% probability to change into shrub land. The change of crop land into built-up may be attributed to the demand of the habitat by the growing population. Shrub land has 21.97% probability to remain as shrub land and it has 50.47% probability to change into crop land which could be a result of over agricultural practice to meet the demand of food and fodder of the growing population. The built-up also has a probability as high as 96.89% to remain as BL which signifies its stability. Water bodies seems to be highly unstable with 29.68% probability to remain as water body while it has 56.02% probability of changing into crop land which may not however be a true projection of this class except there is an occurrence of drought in the region.

From Table 8b, the deciduous forest showed 1,681,340 number of pixels remains into deciduous forest class while 101,600 and 59,601 pixels of deciduous forest will change into mixed forest and crop

Table 8a. Probability of LULC changes in 2025 in percentage.

2005/2015	DF	MF	CL	BL	SL	Built-up	W
DF	0.6431	0.0389	0.2280	0.0065	0.0797	0.0005	0.0034
MF	0.1492	0.4253	0.2330	0.0090	0.1787	0.0026	0.0021
CL	0.0176	0.0044	0.9233	0.0045	0.0317	0.0117	0.0068
BL	0.0609	0.0354	0.5884	0.0704	0.1979	0.0088	0.0382
SL	0.1608	0.0393	0.5047	0.0413	0.2197	0.0110	0.0231
Built-up	0.0086	0.0056	0.0026	0.0019	0.0072	0.9689	0.0052
W	0.0821	0.0043	0.5602	0.0181	0.0257	0.0127	0.2968

Table 8b. Probability of LULC changes in 2025 in number of pixels.

2005/2015	DF	MF	CL	BL	SL	Built-up	W
DF	1,681,340	101,600	59,601	1704	208,310	1416	8769
MF	48,541	138,349	75,784	2938	58,123	861	693
CL	271,097	67,296	14,260,272	69,370	490,367	182,163	104,505
BL	13,411	7785	129,505	15,490	43,565	1927	8408
SL	191,840	46,927	602,085	49,321	262,087	13,173	27,610
Built-up	1950	1257	593	424	1625	218,705	1164
W	21,452	1131	146,287	4727	6716	3328	77,515

Table 8c. Expected to transition in 2025 in number of pixels.

2005/2015	DF	MF	CL	BL	SL	Built-up	W	2005	2015	Change in 2025 (2005–2015)
DF	1,681,340	101,600	596,011	17,041	208,310	1416	8769	3,095,652	2,027,460	1,068,192
MF	48,541	138,349	75,784	2938	58,123	861	693	212,774	1,680,339	−1467565
CL	271,097	67,296	14,260,272	69,370	490,367	182,163	104,505	14,733,978	11,906,568	2,827,410
BL	13,411	7785	129,505	15,490	43,565	1927	8408	534,785	381,446	153,339
SL	191,840	46,927	602,085	49,321	262,087	13,173	27,610	1,310,155	1,925,122	−614967
Built-up	1950	1257	593	424	1625	218,705	1164	111,032	1,949,787	−1838755
W	21,452	1131	146,287	4727	6716	3328	77,515	303,835	494,556	−190721

Note: (−) shows increase whereas (+) shows decrease.

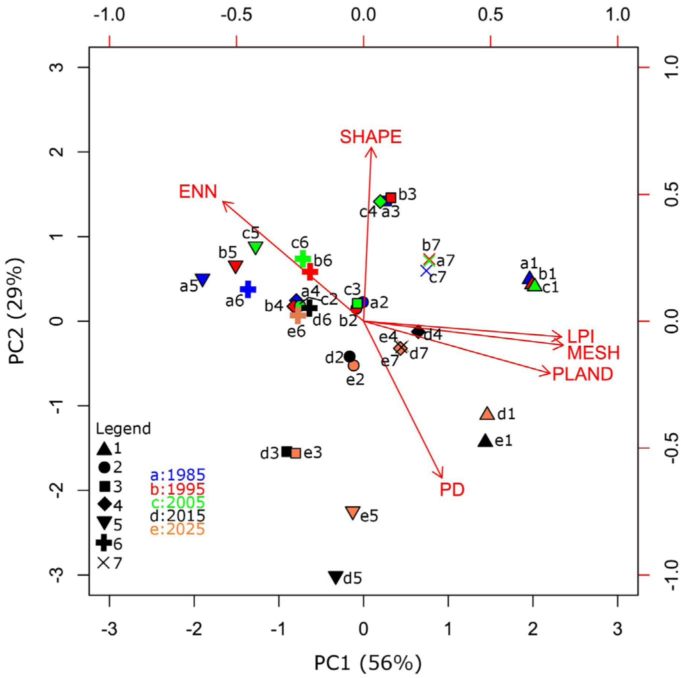

Figure 5. Biplot diagram of landscape metrics of Ton basin (Legend: 1: crop, 2: shrub, 3: water body, 4: barren, 5:built-up, 6: mf, 7: df; blue: 1985; red: 1995; green: 2005; d: 2015; coral: 2025).

Table 9. Rotated component matrix of the landscape metrics.

Landscape metrics	PC1	PC2
MESH	**0.983**	−0.119
LPI	**0.974**	−0.078
PLAND	**0.918**	−0.257
ENN	**−0.692**	0.491
SHAPE	0.039	**0.855**
PD	0.385	**−0.772**
Variance explained	56.4%	29.4%

land, respectively, up to 2025. This is due to increasing population pressure in the area. The mixed forest 138,349 pixel will remain in the mixed forest class while 693 pixels will change into water bodies. The crop land 14,260,272 pixels will remain in the crop land class while 104,505 and 182,163 pixels will change into water bodies and built-up. The barren land showed that 15,490 pixels will remain in the same class while 43,565 pixels will change into shrub land class. Shrub land showed that 262,087 pixels will remain in the same class while 602,085 pixels will transforms into crop land. The built-up showed that 218,705 pixels will remain intact. The water bodies 77,515 pixels will remain in water bodies and only 146,287 pixels will change into crop land. There could be some uncertainty in prediction might be due to imagery quality, classification error and resolution of the sensors (Singh et al. 2015). Table 8c show the expected to transition in 2025 in number of pixels from 2015.

6.4. *Fragmentation analysis and trends of land cover change*

PCA explained 85.8% of the total variance. LPI, MESH and PLAND were in strong positive correlation and in strong negative correlation with ENN (Figure 5) and these metrics formed PC1 accounting for the 56.4% of the variance. SHAPE and PD correlated with each other and formed PC2 accounting for the 29.4% of the variance (Table 9). Usually, values of landscape metrics composed groups for the dates of 1985–1995–2005–2015 in most land cover types (except water bodies). However, from 2005 to 2025 a large increase can be predicted along the axis of PD and SHAPE metrics especially in case of built-up areas and water bodies. It means that while built-up areas increase, patches density and shape index decrease, i.e. smaller water bodies can disappear. Water bodies' area (including its proportion and largest patches and effective mesh size) will decrease while ENN increases and PD also decreases. Area of barren land is predicted to increase.

7. Conclusions

The main advantage of this work is to integrate the land use change modelling with fragmentation for better understanding of the land use/land cover change and fragmentation of the land cover classes. Majority of the studies focused on application of CA–Markov Model to predict the plausible future. Satellite derived land use land cover maps (1985, 1995, 2005 and 2015), biophysical and socio-economic data were used in CA–Markov modelling to know the plausible future land use/land cover area of the region. Model calibration justified that the accuracy (83%) is appropriate for prediction. The CA–Markov model simulated future LULCC up to 2025 by projecting an increase in built up/barren land areas. Results also indicate that if the current LULC trends continues without implementation of holistic sustainable development policies by participation of all the stakeholders, it can affect the rural sustainability. PCA pointed on the trend of changes of class level landscape metrics: modelled data reflected the general decrease in patch density (PD) and shape complexity (SHAPE), and the stagnation of fragmentation (MESH), largest patches (LPI) and nearest distances (ENN). The future knowledge about the land fragmentation will help in protecting the natural resources. In light of land degradation problems in a country like India, the simulated future LULC maps may provide a strategic guide to rural land use planning, effective efforts to reduce deforestation. Furthermore, the simulated future LULC maps can serve as an early warning system of the future effects of LULCC while the model has successfully simulated future LULCC. The biophysical factors of Tons river basin includes namely local micro meteorology (climate and weather), topography, bedrock and soil type, type of vegetation, cropping pattern, surface water and groundwater. The socio-economic drivers determines the choice of land use and decisions to change it are influenced by the size of the household, age, gender, education, employment, attitudes, values and personal traits of household members, site-specific conditions – accessibility and migration. LULCC will depend, on the dynamic relationships among these factors, thus future study should attempt to identify the types of relationship and also to include policy-related factors in the simulation of future LULCC.

Acknowledgements

Authors express their sincere thanks to USGS (http://www.usgs.gov/) for providing satellite data at no cost, volunteer reviewers and the editor of the journal.

Disclosure statement

No potential conflict of interest was reported by the authors.

Funding

This work was supported by the University Grants Commission, New Delhi, India [grant number F. No. 42-74/2013 (SR)]. Szabo S. was supported by the University of Debrecen (RH/751/2015).

References

Ademiluyi IA, Otun WO. 2009. Spatial decision support systems (SDSS) and sustainable development of the third world. J Sustain Dev Africa. 10(4):200–217.

Anderson JR, Hardy EE, Roach JT, Witmer RE. 1976. A land use and land cover classification system for use with remote sensor data Geological Survey Professional Paper 964. Washington (DC): United States Government Printing Office.

Araya YH, Pedro Cabral P. 2010. Analysis and modeling of urban land cover change in Setúbal and Sesimbra. Remote Sens. 2:1549–1563. doi:10.3390/rs2061549.

Bacani VM, Sakamoto AY, Quénol H, Vannier C, Corgnec S. 2016. Markov chains – cellular automata modeling and multicriteria analysis of land cover change in the Lower Nhecolândia subregion of the Brazilian Pantanal wetland. J Appl Remote Sens. 10(1):016004–016020. doi:10.1117/1.JRS.10.016004.

Basommi LP, Qing-feng G, Dan-dan C, Singh SK. 2016. Dynamics of land use change in a mining area: a case study of Nadowli District. J Mt Sci. 13(4):633–642.

Behera MD, Borate SN, Panda SN, Behera PR, Roy PS. 2012. Modelling and analyzing the watershed dynamics using Cellular Automata (CA)-Markov model – A geo-information based approach. J Earth Syst Sci. 121:1011–1024.

Bogyó D, Magura T, Simon E, Tóthmérész B. 2015. Millipede (Diplopoda) assemblages alter drastically by urbanisation. Landscape Urban Plann. 133:118–126. doi:10.1016/j.landurbplan.2014.09.014.

Carr DL. 2004. Proximate population factors and deforestation in tropical agricultural frontiers. Popul Environ. 25(6):585–612. doi:10.1023/B:POEN.0000039066.05666.8d.

Carr DL, Suter L, Barbieri A. 2005. Population dynamics and tropical deforestation: state of the debate and conceptual challenges. Popul Environ. 27(1):89–113. doi:10.1007/s11111-005-0014-x.

Chen Q. 2006. Cellular automata and artificial intelligence in ecohydraulics modelling. Balkema: Taylor & Francis Group. www.taylorandfrancis.CompanyUK.

Chomitz KM, Buys P, De Luca G, Thomas ST, Wertz-Kanounnikoff S. 2007. At loggerheads? Agricultural expansion, poverty reduction, and environment in the tropical forests. A world bank policy research report. Washington (DC): The World Bank.

Congalton RG, Green K. 1999. Assessing the accuracy of remotely sensed data: principles and practices. Boca Raton (FL): CRC Press.

Deák B, Valkó O, Török P, Tóthmérész B. 2016. Factors threatening grassland specialist plants – a multi-proxy study on the vegetation of isolated grasslands. Biol Conserv. 204:255–262. doi:10.1016/j.biocon.2016.10.023.

DeFries RS, Rudel T, Uriarte M, Hansen M. 2010. Deforestation driven by urban population growth and agricultural trade in the twenty-first century. Nature Geoscience. 3:178–181. doi:10.1038/ngeo756.

Eastman JR. 2009. IDRISI help system. Accessed in IDRISI Selva. Worcester (MA): Clark University.

Finenko GA, Anninsky BE, Romanova ZA, Abolmasova GI, Kideys AE. 2001. Chemical composition, respiration and feeding rates of the new alien ctenophore, Beroe ovata, in the Black Sea. Hydrobiologia. 451:177. doi:10.1023/A:1011819819448.

Geist HJ, Lambin EF. 2002. Proximate Causes and Underlying Driving Forces of Tropical Deforestation. Bioscience. 52:143–150.

Guan D, Li HF, Inohae T, Su W, Nagaie T, Hakao K. 2011. Modeling urban land use change by the integration of cellular automaton and Markov model. Ecol Model. 222:3761–3772.

Herold M, Liu X, Clarke KC. 2003. Spatial metrics and image texture for mapping urban land use. Photogramm Eng Remote Sens. 69:991–1001.

Irwin EG, Jayaprakash C, Munroe DK. 2009. Towards a comprehensive framework for modeling urban spatial dynamics. Landscape Ecol. 24(9):1223–1236.

Jha S, Bawa KS. 2006. Population growth, human development, and deforestation in biodiversity hotspots. Conserv Biol. 20:906–912. doi:10.1111/j.1523-1739.2006.00398.x.

Jiang H, Eastman JR. 2000. Application of fuzzy measures in multi-criteria evaluation in GIS. Int J Geograph Inform Sci. 14(2):173–184.

Jokar Arsanjani J, Kainz W, Mousivand AJ. 2011. Tracking dynamic land-use change using spatially explicit Markov Chain based on cellular automata: the case of Tehran. Int J Image Data Fusion. 2(4):329–345.

Jokar Arsanjani J, Helbich M, Kainz W, Darvishi Boloorani A. 2013. Integration of logistic regression, Markov chain and cellular automata models to simulate urban expansion. Int J Appl Earth Observ Geoinform. 21:265–275.

Jolliffe I. 2002. Principal component analysis. New York (NY): Springer.

Kumar N, Singh SK, Srivastava PK, Narsimlu B. 2017. SWAT Model calibration and uncertainty analysis for streamflow prediction of the Tons River Basin, India, using Sequential Uncertainty Fitting (SUFI-2) algorithm. Model Earth Syst Environ. 3:30. doi:10.1007/s40808-017-0306-z.

Kamusoko C, Aniya M, Adi B, Manjoro M. 2009. Rural sustainability under threat in Zimbabwe – simulation of future land use/cover changes in the Bindura district based on the Markov-cellular automata model. Applied Geography. 29(3):435–447.

Lambin EF, Turner BL, Geist HJ, Agbola SB, Angelsen A, Bruce JW, Coomes OT, Dirzo R, Fischer G, Folke C, et al. 2001. The causes of land-use and land-cover change: moving beyond the myths. Global Environ Change. 11:261–269.

Lamine S, Petropoulos GP, Singh SK, Szilárd S, Bachari NEl I, Srivastava PK, Suman S. 2017. Quantifying land use/land cover spatio-temporal landscape pattern dynamics from Hyperion using SVMs classifier and FRAGSTATS®. Geocarto Int. doi:10.1080/10106049.2017.1307460.

Malczewski J. 2004. GIS-based land-use suitability analysis: a critical overview. Progress Plann. 62(1):3–65.

McGarigal K, Marks BJ. 1995. Spatial pattern analysis program for quantifying landscape structure. General Technical Report PNW-GTR-351 US Department of Agriculture, Forest Service, Pacific Northwest Research Station.

McGarigal K, Cushman SA, Neel MC, Ene E. 2002. FRAGSTATS: spatial pattern analysis program for categorical maps Amherst: Computer software program produced by the authors at the University of Massachusetts. http://www.umass.edu/landeco/research/fragstats/fragstats.html

Memarian H, Balasundram SK, Talib JB, Sung CTB, Sood AM, Abbaspour K. 2012. Validation of CA-Markov for simulation of land use and cover change in the langat basin, Malaysia. J Geograph Inform Syst. 542–554: doi:10.4236/jgis.2012.46059.

Meyfroidt P, Lambin EF, Erb KH, Hertel T. 2013. Globalization of land use: distant drivers of land change and geographic displacement of land use. Curr Opin Environ Sustainabil. 5:438–444. doi:10.1016/j.cosust.2013.04.003.

[NRSC] National Remote Sensing Centre. 2014. Land use/land cover database on 1:50,000 scale. LUCMD, LRUMG, RSAA, National Remote Sensing Centre, ISRO. Hyderabad: Natural Resources Census Project.

O'Sullivan D. 2001. Graph-cellular automata: a generalised discrete urban and regional model. Environ Plann B. 28(5):687–705.

Pontius RG Jr. 2000. Statistical methods to partition effects of quantity and location during comparison of categorical maps at multiple resolutions. Photogramm Eng Remote Sens. 68(10):1041–1050.

Pontius RG Jr, Schneider LC. 2001. Land-cover change model validation by an ROC method for the Ipswich watershed, Massachusetts, USA. Agri Ecosyst Environ. 85(1–3):239–248.

Saaty TL. 1980. The analytical hierarchy process. New York (NY): McGraw Hill.

Semwal RL. 2005. The Terai Arc landscape in India, securing protected areas in the face of global change. New Delhi: WWF-India.

Singh SK, Singh CK, Mukherjee S. 2010. Impact of land-use and land-cover change on groundwater quality in the Lower Shiwalik hills: a remote sensing and GIS based approach. Cent Eur J Geosci. 2(2):124–131. doi:10.2478/v10085-010-0003-x.

Singh SK, Kumar KS, Aier B, Kanduri VP, Ahirwar S. 2012. Plant community characteristics and soil status in different land use systems in Dimapur district, Nagaland, India. For Res Pap. 73:305–312.

Singh SK, Srivastava PK, Gupta M, Thakur JK, Mukherjee S. 2013. Appraisal of land use/land cover of mangrove forest ecosystem using support vector machine. Environ Earth Sci. 1–11.

Singh SK, Pandey AC, Singh D. 2014. Land use fragmentation analysis using remote sensing and fragstats. In: Srivastava PK, Gupta M, Mukherjee S, Islam T, editors. Remote sensing applications in environmental research Society Earth Science Ser; p. 151–176.

Singh SK, Mustak S, Srivastava PK, Szabó S, Islam T. 2015. Predicting spatial and decadal LULC changes through cellular automata Markov chain models using earth observation datasets and geo-information. Environ Process. 2:61–78.

Singh SK, Srivastava PK, Szilárd S, Petropoulos GP, Gupta M, Islam M. 2016. Landscape transform and spatial metrics for mapping spatiotemporal land cover dynamics using Earth Observation data-sets. Geocarto Int. 1–15. doi:10.1080/10106049.2015.1130084.

Soe WM, Le W. 2006. Multicriteria decision approach for land use and land cover change using Markov chain analysis and a cellular automata approach. Canadian J Rem Sens. 32:390–404.

Solomon G, Woldeamlak B, Gärdenäs AI, Bishop K. 2014. Forest cover change over four decades in the Blue Nile Basin, Ethiopia: comparison of three watersheds. Reg Environ Change. 14:253–266.

Srinivasan NT. 2001. Economic reforms and global integration. Working Paper No 120. Stanford (CA): Stanford University. (http://scid.stanford.edu/sites/default/files/publications/120wp.pdf).

Srivastava PK, Singh SK, Gupta M, Thakur JK, Mukherjee S. 2013. Modeling impact of land use change trajectories on groundwater quality using Remote Sensing and GIS. Environ Eng Manag J. 12:2343–2355.

Srivastava PK, Mukherjee S, Gupta M, Islam T. 2014. Remote sensing applications in environmental research. New york (NY): Springer Verlag . ISBN 978-3-319-05905-1.

Srivastava PK, Han D, Rico-Ramirez MA, Bray M, Islam T. 2012. Selection of classification techniques for land use/land cover change investigation. Advances in Space Research. 50:1250–1265.

Steeb WH. 2011. The nonlinear workbook: chaos, fractals, cellular automata, neural networks, genetic algorithms, gene expression programming, support vector machine, wavelets, hidden markov models, fuzzy logic with c++, java and symbolicc++ programs. Singapore: World Scientific.

Szabó S, Csorba P, Szilassi P. 2012. Tools for landscape ecological planning – scale, and aggregation sensitivity of the contagion type landscape metric indices. Carpathian J Earth Environ Sci. 7:127–136.

Temesgen G, Taffa T, Mekuria A. 2017. Erosion risk assessment for prioritization of conservation measures in Geleda watershed, Blue Nile basin, Ethiopia. Environ Syst Res. 6(1):1–14.

Wadia DN. 1975. Geology of India. 4th ed. New Delhi: Tata Mcgraw Hill; p. 508.

Wang Y, Zhang X. 2001. A dynamic modeling approach to simulating socioeconomic effects on landscape changes. Ecol Model. 140(1):141–162.
Wu F. 2002. Calibration of stochastic cellular automata: the application to rural-urban land conversions. Int J Geograph Inform Sci. 16(8):795–818.
Wu F, Webster CJ. 2000. Simulating artificial cities in a GIS environment: urban growth under alternative regulation regimes. Int J Geograph Inform Sci. 14(7):625–648.
Yadav SK, Singh SK, Gupta M, Srivastava PK. 2014. Morphometric analysis of Upper Tons Basin from Northern Foreland of Peninsular India using CARTOSAT Satellite and GIS. Geocarto Int. 1–20. doi:10.1080/10106049.2013.868043.
Yang X, Zheng XC, Chen R. 2014. A land use change model: integrating landscape pattern indexes and Markov-CA. Ecol Model. 283:1–7.
Yulianto F, Prasasti I, Pasaribu JM, Fitriana HL, Haryani NS, Sofan P. 2016. The dynamics of land use/land cover change modeling and their implication for the flood damage assessment in the Tondano watershed, North Sulawesi. Model Earth Syst Environ. 2:1–20. doi:10.1007/s40808-016-0100-3.